

OPTIMAL DAMPING OF SERVO AXIS USING GRÖBNER BASES

EKKEHARD BATZIES, LUKAS KATTHÄN, VOLKMAR WELKER, AND OLIVER ZIRN

ABSTRACT. We present a new and algebraic approach to the optimal damping of servo axes during commissioning. The approach is based on control of root loci of the denominator of the transfer function using Gröbner bases techniques. The results are either explicit formulas for simple systems or descriptions of the optima via roots of univariate polynomials. The power of the result is demonstrated in examples.

1. INTRODUCTION

1.1. Servo controller commissioning. Servo axis commissioning is one of the main issues for the setup procedure of production machines and machine tools. In feedback control theory, very few practically applicable commissioning rules for servo axes have been developed up to now (see [1, 7, 11]). The heuristic commissioning procedures proposed by the automation system manufacturers [6] require multiple measurements and – especially for axes with flexible mechanical structure – are quite time consuming. Due to the lack of commissioning time, most of the production machines operate with deficient servo axis performance with disadvantageous effects on productivity and utilization of energy.

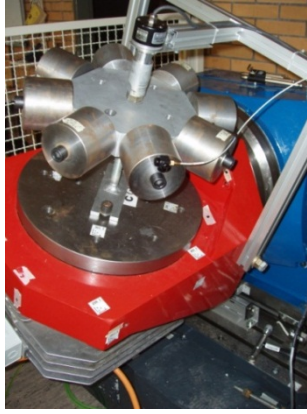
The main parameter for position controlled servo drives is the velocity feedback proportional gain K_P [13]. On one hand, the velocity control loop has to be fast enough (i.e. high K_P) to achieve a satisfactory feedback control performance in the position control loop. On the other hand, the velocity control loop is essential for vibration damping of the flexible mechanical structure. From the engineering point of view, it is highly desirable to assess the velocity control gain K_P directly from formulas or through a mathematical description that allows a simple analysis of its dependency on the parameters. These rules should be based on the control topology as well as on plant parameters that are easy to identify. In this paper we propose a method to derive rules of this type using elimination methods from polynomial algebra, in particular we apply Gröbner bases techniques.

As an example we describe the engineering problem in the mathematically least complex *standard case* of a servo motor with flexible load shown in Figure 1a. The plant parameters [15], complete inertia Θ , inertia ratio λ and resonant frequency ω_0 can be identified e.g. by a measured drive frequency response [12, 15]. The transfer function for the velocity control loop of the physical model in Figure 1b is given by (see [14]):

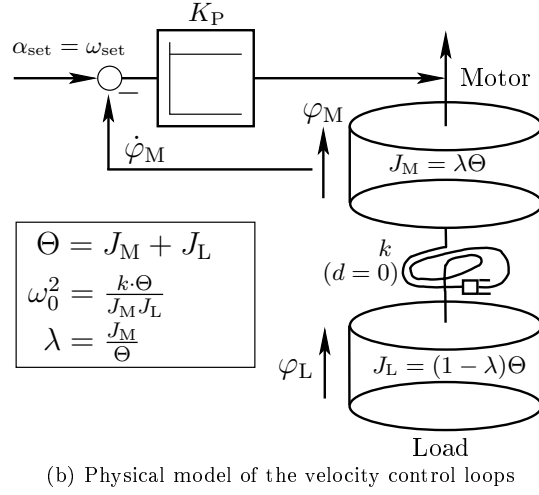
$$(1) \quad G(s) = \frac{\dot{\varphi}_M(s)}{\dot{\alpha}_{\text{set}}(s)} \stackrel{\kappa = \frac{K_P}{\Theta}}{=} \frac{\frac{\kappa}{\lambda} \cdot s^2 + \omega_0^2 \cdot \kappa}{s^3 + \frac{\kappa}{\lambda} \cdot s^2 + \omega_0^2 \cdot s + \omega_0^2 \cdot \kappa}$$

Date: October 16, 2012.

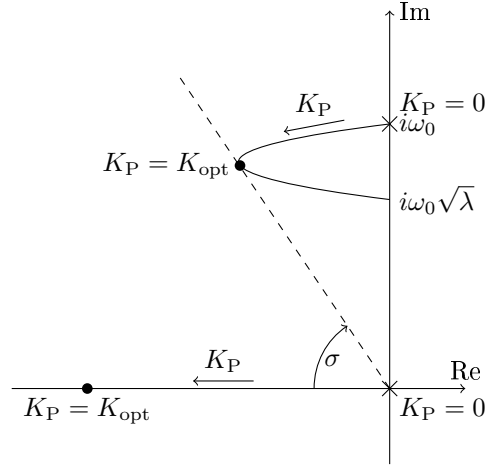
This work was supported by the DFG grant ZI 1301/1-1.



(a) Test bench (machine tool laboratory of the Swiss Federal Institute of Technology)



(b) Physical model of the velocity control loops



(c) Root locus for the feedback controller gain K_P

Figure 1: Rotary servo axis (C-axis) with flexible load

The root locus for that transfer function in Figure 1c elucidates the optimization problem for the gain K_P . Low K_P values result in a slow system with poor damping, very high K_P values decrease the damping of the complex poles too. The optimum setting will have minimum damping angle σ . Although a numerical optimization of K_P for optimum damping is quite simple to implement, e.g. in Matlab [12, 15], a rigorous analytic solution $K_{p,opt}(\Theta, \lambda, \omega_0)$ for this engineering problem is desirable, since it avoids non-trivial numerical approximations but also allows an understanding to the behavior of the optimum in terms of the system parameters.

1.2. Previous work. The commissioning of PI or state space velocity feedback control loops has been discussed since decades [1, 3, 5, 7, 9, 11]. Up to now, the commissioning rules are almost exclusively based on root locus optimization as

shown in Figure 1c. In the known approaches the root locus analysis requires either engineering tools that are well suited for research laboratories and educational test benches, but not for the dirty and noisy manufacturing environment or numerical optimization which does not yield insight in the dependency of the optimum on the system parameters and raises questions on convergence and feasibility. Rules based on explicit analytic formulas or simple numerical algorithms, such as finding root loci of polynomials in one variable, seem more suitable. A first attempt described for specific cases in [15] and [2] derives rules of thumb out of intensive parameter studies by rough and intuitive engineering approximations from data provided by numerical optimization (for the case described in Figure 1). Although these first rules of thumb are only empirical approximations, their practical use for the axis commissioning at different industrial partners was quite encouraging. A first thorough analytic solution for the case treated in Figure 1 was given in [2]. This work was already based on Gröbner bases techniques, but the actual derivation and method were not presented in [2]. It was the starting point for research on a more refined use of Gröbner bases for this purpose. This paper presents the results of these efforts.

It is a contribution to the development of rigorous rules for dominating parameters in system topologies (as given in Section 4) which together with system parameter identification (e.g. by measured plant frequency response interpretation) is the crucial precondition for (semi-)automatic servo axis controller commissioning and optimization.

1.3. Outline of the paper. In Section 1 we introduce the basic engineering setting and provide a concrete example. We outline the contribution made by the paper and survey the existing approaches. Then in Section 2.1 the mathematical model is introduced and in Section 2.2 the algebraic tools of Gröbner bases and resultants are briefly explained without going into much detail. In Section 2.3 a first application of the algebraic approach is given. Here a Gröbner technique for the extraction of the transfer function from physical descriptions of the system is outlined. Then in Section 3 our principal method is described concretely in case of systems of degree 3, 4 and 5. Then in Section 4 the results of the method for several concrete systems are provided. Finally in Section 5 the contribution of the paper is validated and discussed and an outlook is given.

2. MATHEMATICAL MODELS

2.1. Our Model. We consider a mechanical system whose state at time t can be described by a state vector $\mathbf{x}(t) = (x_1(t), \dots, x_n(t)) \in \mathbb{R}^n$. Moreover, we have a real valued input function $u(t)$ which models our control of the system and a real valued output function $y(t)$. The dynamics of the system is then given by the following equations of motion:

$$(2) \quad \frac{d}{dt}\mathbf{x}(t) = \mathbf{A}\mathbf{x}(t) + \mathbf{b}u(t)$$

$$(3) \quad y(t) = \mathbf{c}^t\mathbf{x}(t)$$

Here $\mathbf{A} \in \mathbb{R}^{n \times n}$ is the *state matrix*, $\mathbf{b} \in \mathbb{R}^n$ is the *control vector* and $\mathbf{c} \in \mathbb{R}^n$ is the *output vector*. In the literature, one often considers systems with more than one input and one output variable. In that case \mathbf{b} and \mathbf{c} are replaced by matrices of the appropriate size. However, in this paper we restrict ourselves to the case of one input variable and one output variable.

In general, solutions $\mathbf{x}(t)$ to (2) are a superposition of solutions of the homogeneous system $\frac{d}{dt}\mathbf{x}(t) = \mathbf{A}\mathbf{x}(t)$ and a fixed special solution of (2). The solutions $x_{\text{hom}}(t)$ of the homogeneous system are all of the form

$$\mathbf{x}_{\text{hom}}(t) = e^{(x+iy)t}\mathbf{x}_0,$$

where $x, y \in \mathbb{R}$ and i is the imaginary unit. In practice, it is desirable that for $t \rightarrow \infty$ the solutions to the homogeneous system approach zero as fast as possible, as they represent transient behaviour of the system. In particular, we should have that $x < 0$. The occurring exponents $x + iy$ are the eigenvalues of \mathbf{A} and thus the zeros of the *characteristic polynomial*

$$\mathcal{P}_A(s) = \det(s\mathbf{E} - \mathbf{A})$$

where $\mathbf{E} \in \mathbb{R}^{n \times n}$ denotes the identity matrix. We write $\sigma = \frac{y}{x}$ for the ratio of the imaginary and real part of a non-real zero. Since we consider a minimization problem we chose the negative imaginary part y from the pair of conjugate roots. Then we can write

$$\mathbf{x}_{\text{hom}}(t) = e^{(1+i\sigma)x t}\mathbf{x}_0.$$

Thus, σ determines the shape of the function, while x is a time constant.

In our case, the state matrix \mathbf{A} depends on a parameter a . Our goal is to determine a value of a , such that the zeros of $\mathcal{P}_A(s)$ are “optimally” located in the complex plane. Experimental data suggests that the optimal location is achieved when minimizing the value of σ . Hence for our purposes we need to solve the following optimization problem:

Let $\mathcal{P}(s; a) = s^r + c_1(a)s^{r-1} + \dots + c_r(a)$ be a polynomial in the variable s whose coefficients $c_i(a)$ are real functions depending on a real variable a . Let $x_1(a)(1 + i\sigma_1(a)), \dots, x_r(a)(1 + i\sigma_r(a))$ be the complex zeros of $\mathcal{P}(s; a)$.

Determine a value of a that minimizes the maximum of the $\sigma_i(a)$, with respect to the constraint $x_i(a) \leq 0$ for $1 \leq i \leq r$

Indeed, in our application the $c_i(a)$ will also depend on additional parameters q_1, \dots, q_m . It will be a polynomial in a and a rational function in q_1, \dots, q_m .

Another interpretation of the characteristic polynomial can be given in terms of the *transition function*. For this we consider the Fourier transformation of (2):

$$\begin{aligned} i\omega\hat{\mathbf{x}}(\omega) &= \mathbf{A}\hat{\mathbf{x}}(\omega) + \mathbf{b}\hat{u}(\omega) \\ \hat{y}(\omega) &= \mathbf{c}^t\hat{\mathbf{x}}(\omega) \end{aligned}$$

We can eliminate $\hat{\mathbf{x}}(\omega)$ from this system and write $\hat{y}(\omega) = \mathbf{c}^t(i\omega\mathbf{E} - \mathbf{A})^{-1}\mathbf{b}\hat{u}(\omega)$ where $\mathbf{E} \in \mathbb{R}^{n \times n}$ denotes the identity matrix. The *transition function* of the system is then defined by

$$G(s) := \mathbf{c}^t(s\mathbf{E} - \mathbf{A})^{-1}\mathbf{b}.$$

This is a rational function in s which describes the dependence of the output $u(t)$ from the input $y(t)$. In general, its denominator is a divisor of the characteristic polynomial. However, in most cases of practical relevance, these two polynomials are equal. If they are not equal, then the additional zeros of the characteristic polynomial correspond to homogeneous solutions that cannot appear with the given input vector \mathbf{b} . For example, for a Master-Slave drive (see Case 3 below), there are

two additional zeros of the characteristic polynomial. They correspond to asymmetric oscillations which are suppressed by the symmetry of the model. In this situation, we will consider the denominator of the transition function rather than the characteristic polynomial.

2.2. Eliminations Methods. In this subsection, we shortly recall the two eliminations methods used in this paper, Gröbner Bases and resultants; see [4, Chap. 3] for a more detailed treatment. Consider a system of polynomial equations

$$(4) \quad p_1(x_1, \dots, x_n) = p_2(x_1, \dots, x_n) = \dots = p_m(x_1, \dots, x_n) = 0$$

for polynomials $p_1, \dots, p_m \in \mathbb{C}[x_1, \dots, x_n]$. In our applications we will be interested in a subset of the coordinates of the solutions of the system in \mathbb{C}^n . Say we are interested in the coordinates x_1, \dots, x_l for some $l \leq n$.

Gröbner Bases: Computing a Gröbner Basis with respect to an *elimination ordering* gives a new polynomial system

$$(5) \quad \tilde{p}_1(x_1, \dots, x_n) = \tilde{p}_2(x_1, \dots, x_n) = \dots = \tilde{p}_{\tilde{m}'}(x_1, \dots, x_n) = 0$$

such that the solution sets of (4) and (5) coincide. After suitable numbering the new system now is divided into two subsystems:

$$(6) \quad \tilde{p}_1(x_1, \dots, x_n) = \tilde{p}_2(x_1, \dots, x_n) = \dots = \tilde{p}_{\tilde{m}''}(x_1, \dots, x_n) = 0$$

and

$$(7) \quad \tilde{p}_{\tilde{m}''+1}(x_1, \dots, x_n) = \tilde{p}_{\tilde{m}''+2}(x_1, \dots, x_n) = \dots = \tilde{p}_{\tilde{m}'}(x_1, \dots, x_n) = 0$$

where (6) contains the (possibly empty) set of polynomials from (5) which lie in $\mathbb{C}[x_1, \dots, x_l]$. The crucial property of the two systems is:

Almost every solution of (6) can be extended to a solution of (5) or equivalently (4); see [4, Chap. 3, Theorem 3]. In other words, we have eliminated the variables x_{l+1}, \dots, x_n .

Resultant: First consider the special case where we have only two polynomials p_1, p_2 and we want to eliminate only one variable x_n . The *resultant* $\text{Res}_{x_n}(p_1, p_2)$ is a polynomial that depends on the same set of variables as p_1 and p_2 except x_n . Similar to the Gröbner basis method we have the property that almost every zero of $\text{Res}_{x_n}(p_1, p_2)$ can be extended to a common zero of p_1 and p_2 (under certain assumptions). We refer to [4, Chap. 3, ¶6] for exact definitions and basic properties of resultants. For the elimination of several variables from a set of polynomials the resultant method can be applied iteratively, but this can easily lead to an explosion of the polynomial degrees.

In our application, the resultant turned out to be faster than Gröbner Basis elimination for the elimination of a single variable. Nevertheless, since we also need to eliminate several variables at once Gröbner bases methods are essential for our work.

2.3. Extracting the polynomial equations using Gröbner Bases. In practice, the equations of a system are sometimes given in a form different from our standard form (2). For instance, they may be given by some basic relations between the state variables and some additional relations describing effect of the input on the system. Even though in general it is mathematically not too difficult to manually transform these equations into the standard form (2), it is tedious and fault prone. Therefore, it is convenient to replace the manual derivation by computer

algebra tools which will be our first use of the elimination methods from Section 2.2. Next we describe an algorithm to determine the transition function:

We first substitute every differential $\frac{d}{dt}$ in the equations by a new variable s ; this amounts to performing a Laplace transformation. Then we add the additional equation $y = Gu$ to the system, where we treat G as a variable. Before we can solve this system of equations for G , we need to exclude the case that $u = 0$, because this corresponds to a trivial solution. This can be done by *saturating* with respect to u , see Chap. 2.2 of [10]. Next we use the elimination methods from Section 2.2 (and a computer algebra system) to eliminate u , y and the state variables from the system to get an expression for G in terms of s . Then solving for $G = G(s)$ yields the transition function.

As an example, we derive (1) from the physical relations of the velocity control loop on Figure 1b. The (Laplace transformed) equations of motion are the following:

$$(8a) \quad J_M \cdot \varphi_M \cdot s^2 = -k(\varphi_M - \varphi_L) + M$$

$$(8b) \quad J_L \cdot \varphi_L \cdot s^2 = k(\varphi_M - \varphi_L)$$

In addition, we have the equation of the velocity control and for the transition function:

$$(8c) \quad M = K_P(\alpha_{\text{set}} - \varphi_M s)$$

$$(8d) \quad \varphi_M \cdot s = G \cdot \alpha_{\text{set}}$$

Saturation with respect to α_{set} yields two additional equations:

$$(8e) \quad J_L \cdot K_P \cdot s^2 + kK_P = (J_M J_L s^3 + J_L K_P s^2 + (J_M + J_L)ks + kK_P)G$$

$$(8f) \quad 0 = G \cdot s(\varphi_M J_M + \varphi_L J_L) + (G - 1) \cdot \varphi_M \cdot K_P$$

We eliminate the variables φ_M, φ_L, M and α_{set} from the equations (8a) – (8f) and solve for G to obtain

$$G = \frac{J_L \cdot K_P \cdot s^2 + k \cdot K_P}{J_M \cdot J_L \cdot s^3 + J_L \cdot K_P \cdot s^2 + k(J_M + J_L)s + k \cdot K_P}.$$

By the substitutions indicated in Figure 1b, this is equivalent to (1). The reader may notice that in this example one could have read off the expression for G from (8e) without using elimination. Unfortunately, this coincidence happens in this basic example. More complicated examples do not bear this feature but are technically too involved to serve as an example for the principle approach.

3. OUR METHOD

Let $\mathcal{P} = \mathcal{P}(s, a; q_1, \dots, q_m)$ denote the characteristic polynomial. Here, s is the polynomial variable, a is the parameter to optimize and q_1, \dots, q_m are further parameters. In our algebraic approach we consider the additional parameters q_1, \dots, q_n as variables. We distinguish the case when the characteristic polynomial \mathcal{P} has degree 3 in s and the case of degree 4 or 5 in s .

3.1. Degree 3. Consider a general characteristic polynomial of degree 3:

$$s^3 + c_1 s^2 + c_2 s + c_3$$

Since \mathcal{P} has degree 3, we generically expect one real solution and a pair of complex conjugated solutions. Thus, there is only one σ to minimize. We consider the problem over the reals, so at first we substitute $s = x(1 + i\sigma)$ for variables x and

σ in \mathcal{P} . Since algebraic equations cannot force x and σ to be real, by doing so, we increase the number of solutions of the system. Thus at the end we have to discard the irrelevant – non-real – solutions. Separating the real and imaginary parts of \mathcal{P} we obtain two polynomials p_1, p_2 :

$$\begin{aligned} p_1 &= (1 - 3\sigma^2)x^3 + (1 - \sigma^2)c_1x^2 + c_2x + c_3 \\ p_2 &= (3\sigma - \sigma^3)x^3 + 2\sigma c_1x^2 + \sigma c_2x \end{aligned}$$

Now eliminate x from those two polynomials using the resultant to get a third polynomial p_3 . We substitute $\tilde{\sigma} = (\sigma^2 + 1)/4$ to get a more succinct representation. Note that this is a monotone transformation, so a minimum of $\tilde{\sigma}$ corresponds to a minimum of σ . After removing trivial factors we get

$$p_3 = (c_1c_2 - c_3)^2\tilde{\sigma}^3 + (c_1c_2c_3 - 3c_3^2 - c_1^3c_3 - c_2^3)\tilde{\sigma}^2 + (3c_3 + c_1c_2)c_3\tilde{\sigma} - c_3^2$$

We want to minimize $\tilde{\sigma}$ over the real curve $p_3 = 0$ in the $(\tilde{\sigma}, a)$ -plane. For this we employ the method of Lagrange multipliers. This yields a system of equations:

$$(9) \quad p_3(\tilde{\sigma}, a) = 0$$

$$(10) \quad \lambda \frac{\partial}{\partial a} p_3(\tilde{\sigma}, a) = 0$$

$$(11) \quad \lambda \frac{\partial}{\partial \tilde{\sigma}} p_3(\tilde{\sigma}, a) = 1$$

Here, λ is the Lagrange multiplier. It is easy to see that (11) only determines the value of λ . Thus we can safely ignore this equation and concentrate on the remaining two. Of course we can eliminate λ from (10) by division. So we are left with two equations in two variables. Hence we can compute the resultant $p_4 := \text{Res}_{\tilde{\sigma}}(p_3, \frac{\partial}{\partial a} p_3)$ to eliminate $\tilde{\sigma}$. Now we have one polynomial $p_4 = p_4(a)$ and the optimal value of a can be computed by solving $p_4 = 0$.

3.2. Degrees 4 and 5. Polynomials of degree 4 or 5 generically have two pairs of complex roots. Our objective function is then the maximum of the two ratios of real and imaginary parts. We distinguish two cases: In the first case, the root with the higher imaginary/real ratio attains a minimum in a region of the parameter space where the second root uniformly has a lower ratio. In this case one can apply a method analogous to the one described for degree 3. However, the occurring polynomials tend to be very complicated.

In the second case, one pair has an increasing ratio, the other one has a decreasing ratio, and the minimum is obtained in the point where the ratios are equal. In the case that \mathcal{P} is of degree 4 we pursue the following Ansatz: Consider the general polynomial

$$(12) \quad p = (s - x_1(1 + i\sigma))(s - x_1(1 - i\sigma))(s - x_2(1 + i\sigma))(s - x_2(1 - i\sigma))$$

of degree 4 for which the two pairs of roots to have the same ratio σ . We compare its coefficients with the actual \mathcal{P} to get a system of 4 equations in the indeterminates x_1, x_2, σ and a . For the optimal value of a , \mathcal{P} can be written in the form (12). Hence, the optimal $a = a_0$ is part of a solution $(x_{1,0}, x_{2,0}, \sigma_0, a_0)$ of this system of equations. Using Gröbner bases we can eliminate all indeterminates but a . Since the polynomial ring in one indeterminate is a principal ideal domain, this results in exactly one polynomial $p_1 = p_1(a)$. Moreover, $p_1(a)$ is not constant, because there

exists an optimal a , but not all values for a are optimal. Again, we can compute the optimal value of a by solving $p_1(a) = 0$.

For a polynomial of degree 5, we include an additional factor $(s - x_3)$ in our Ansatz and eliminate x_3 in the elimination step. Otherwise we proceed analogous to the degree 4 case.

We are currently working in applying the method for degrees ≥ 6 .

3.3. Remarks. Let us add some technical remarks.

- We note that the ratio σ is invariant under a scaling transformation $s \mapsto \gamma s$ for any $\gamma \neq 0$. The γ may even depend on a . Using this, we were in some cases able to simplify the dependence of \mathcal{P} on a .
- In our second method we do not need to single out a from the other parameters. Instead, we can freely reparametrize \mathcal{P} , thus greatly simplifying the elimination step. Only in the end we need to substitute back to obtain the optimal value of a . We see this as the reason for the fact that in experiments for degree 5 the second method is computationally more tractable than the first one.
- In general, for polynomials of degrees 4 and 5 it is not obvious which case applies. The answer may even depend on the region of the parameter space.
- The computation time needed for the elimination step in the second method depends strongly on the order the variables are eliminated. Our experiments suggest that it is advantageous to eliminate x_3 (in degree 5) first, then x_1 and x_2 , and σ last.

4. CONCRETE CASES

In this section we demonstrate the applicability of the method described in Section 3 in several concrete engineering settings.

Case 1: P-velocity control with structural flexibility. The case given in Figure 1 and Equation (1) represents a complete class of structural flexibilities at machine tools and robots; see [12, p.35]. The optimum damping can be derived by the methods described in Section 3.1. It is given by

$$(13) \quad \kappa = \frac{K_P}{\Theta} = \omega_0 \lambda^{0.75} .$$

Case 2: State space velocity control with delayed input generation. Another dominating influence is the delayed servo motor input generation (i.e. force or torque) due to the inductance and the dead time in the current control loop as well as by input variable filters for noise suppression. As shown in Figure 2, this input delay can be considered by an equivalent delay time constant T , that is displayed on the commissioning software of modern servo drives and control systems.

For typical servo motor delay times ($T = 0.5 - 2$ ms), the effect on the P-velocity control is negligible in comparison to the flexible structure. For state control extensions as shown in Figure 2, the delay time is the dominating restriction for the control performance [12]. Velocity state space controller commissioning is based on the pole placement method following Schröder [9] with one tuning parameter Ω that represents the cut-off frequency of the velocity control loop. The

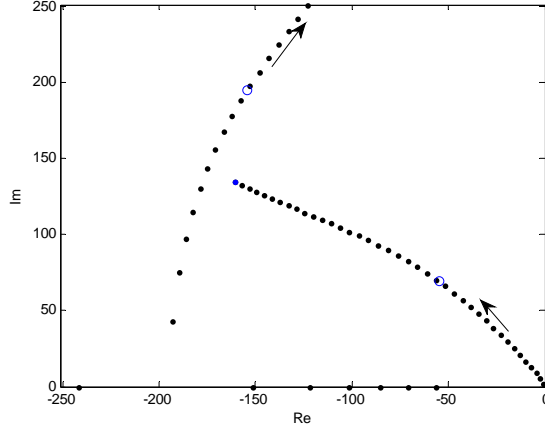
(a) Root locus for the tuning parameter Ω (here $T = 0.3\omega_0^{-1}$)

Figure 2: Delayed input generation

resulting transfer function denominator is

$$s^4 + \frac{1}{T}s^3 + \left(\frac{2\Omega}{T} + \omega_0^2\right)s^2 + \frac{2\Omega^2}{T}s + \frac{\Omega^3}{T}.$$

Optimum damping angle for all poles is reached for

$$(14) \quad \Omega = \frac{1}{4T}.$$

Case 3: Multi drive control. Very large machine tool applications require distributed drives for one axis degree of freedom. Figure 3 shows such a swivelling axis for a large milling machining centre.

Although the physical model in Figure 3b represents a 5th-order system for the velocity control loop, the symmetric velocity control of master and slave drive results in a 3rd-order transfer function:

$$G(s) = \frac{\dot{\varphi}_L(s)}{\dot{\alpha}_{\text{set}}(s)} \stackrel{\kappa = \frac{K_P}{\Theta}}{=} \frac{\frac{2\omega_{01}^2 \kappa}{1-2\lambda}}{s^3 + \frac{\kappa}{\lambda}s^2 + \frac{\omega_{01}^2}{1-2\lambda}s + \frac{2\omega_{01}^2 \kappa}{1-2\lambda}}$$

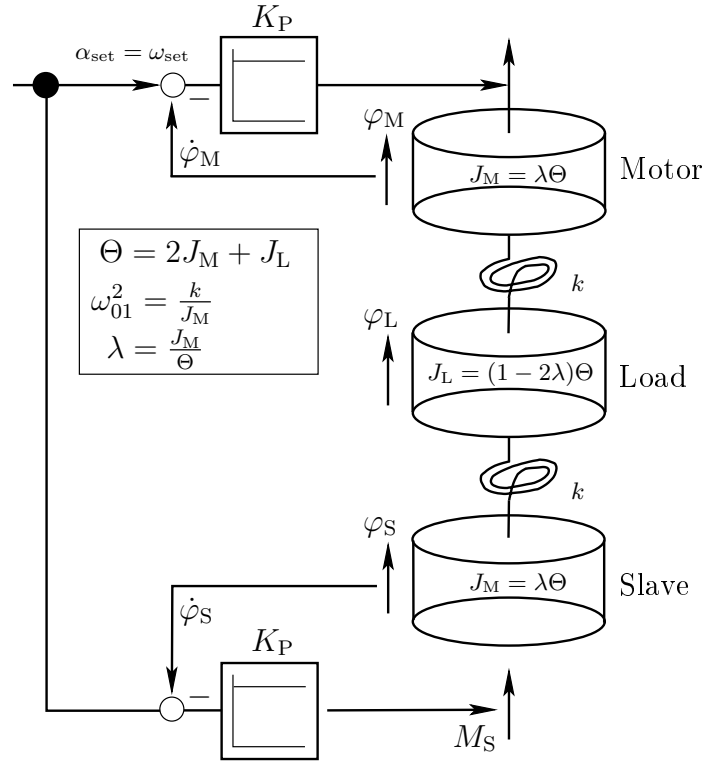
The optimization task shown in Figure 3c is similar to Case 1. Optimum velocity control loop damping is achieved for

$$(15) \quad \kappa = \frac{K_P}{\Theta} = \frac{\omega_{01} \lambda^{0.75}}{\sqrt[4]{2}\sqrt{1-2\lambda}}.$$

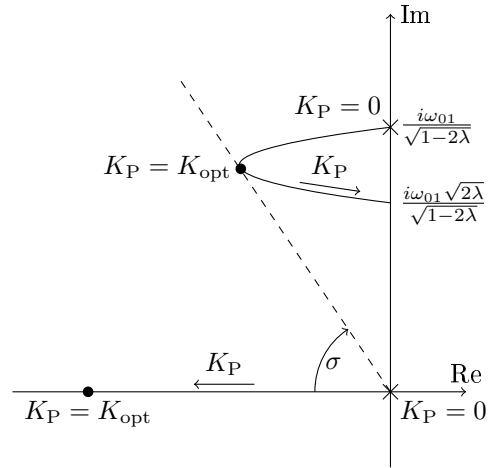
Also here, state space control and delayed input variables result in additional cases for multi drive control. Furthermore, servo axes with two dominating flexible eigenmodes (resonant frequencies), that can be considered as 5th order systems for the velocity control, can be optimized concerning the feedback controlled damping performance. However, in these cases our method does not yield a closed formula for the optimal damping parameter. Instead, we obtain a univariate polynomial of degree 5 or higher, whose real positive zero corresponds to the optimum damping



(a) Milling machine setup (courtesy Rückle GmbH, Römerstein, Germany)



(b) Physical model of the velocity control loops



(c) Root locus for the feedback controller gain K_P

Figure 3: Swivelling axis (B-axis) with master-slave control [8]

Case, Axis	K_P in Nms/rad		
	Analytical rule	Simulation	Measurement
1, C-Axis [12] with P-velocity control $\Theta = 2.9 \text{ kg m}^2$ $\lambda = 0.51$ $\omega_0 = 75 \text{ rad/s}$	Eq. (13): $K_P = 131 \text{ Nms/rad}$	$K_P =$ $120 - 150 \text{ Nms/rad}$	$K_P = 125 \text{ Nms/rad}$
2, C-Axis [12] with state space control $\Theta = 2.9 \text{ kg m}^2$ $\lambda = 0.51$ $\omega_0 = 75 \text{ rad/s}$ $T = 1.8 \text{ ms}$	Eq. (14): $\Omega = 139 \text{ 1/s}$	$\Omega = 125 - 140 \text{ 1/s}$	$\Omega = 135 \text{ 1/s}$
3, B-Axis [8] with master-slave control $\Theta = 806 \text{ kg cm}^2$ $\lambda = 0.33$ $\omega_{01} = 125 \text{ rad/s}$	Eq. (15): $K_P = 6.23 \text{ Nms/rad}$	$K_P = 6 - 7 \text{ Nms/rad}$	$K_P = 6.7 \text{ Nms/rad}$

Table 1: Examples of realistic Servo Axis

parameter. We display the leading term and the constant term of the polynomial for one of the cases we have worked out.

$$p(\Omega) = \sigma_L^5 \Omega^{12} + \dots + \gamma \omega_0^{12} (\gamma + 1 - \sigma_L)^3 (\gamma + 1 - \sigma_L + 4\lambda\gamma\sigma - 4\lambda\sigma_L)^2$$

Since a full presentation of the case covered by the polynomial and a full presentation this degree 12 polynomial would explode the size of this paper, we refrain from a detailed presentation.

5. DISCUSSION OF THE RESULTS AND OUTLOOK

The analytic rules given in Section 4 have been tested at several dozen servo axis commissioning procedures. Table 1 shows three examples of realistic servo axes, that elucidate the fact that the rules yield good starting values for the axis setup. It should be noted that although the analytic rules yield one precise control gain value based on the identified system parameters, there is a certain range of suitable gains in practice. When simulating or measuring the step response of a servo axis velocity controller in the time domain, the commissioning results of different experienced practitioners will vary in the range of 20–40%. Besides the conservatism of the commissioner, the audible drive performance influences the real controller gain adjustment.

We would like to stress two main advantages of the approach presented in this paper.

On the one hand, analytic estimation of the achievable controller gains can replace numerical simulation in the design phase of a new machine tool or robot

servo axis. For numerical simulation, a suitable engineering tool (e.g. MATLAB/Simulink, ANSYS CT, PERMAS etc.) as well as thoroughgoing modelling of the system is required, that can consume hours or days. Also an expensive software license is needed. Although numerical simulation of servo axes is the engineering state of the art, partial replacement of simulation by estimation will make the development process more effective in the design phase. Thus the axis performance can be evaluated based on a numerical modal analysis even if a machine tool only exists as CAD sketch.

On the other hand, analytic controller gain estimation simplifies the commissioning procedure of a servo axis because the required system parameters can be identified by frequency response measurements (as explained in Chapter 1), that can be considered as standard feature for modern servo controllers. Actual (semi-) automatic controller commissioning tools are based on phase and gain margin [6]. Due to the noisy measurement environment at real servo axes, the discrimination of these margins can be quite difficult. However, the detection of the system parameters for the rules of thumb derived in this paper is much easier, even for noisy frequency response measurement displays. The development of a practical automatic commissioning tool for servo axes and its intensive application at several industrial partners is the future focus for the applied research in this project.

REFERENCES

- [1] A. Bahr and S. Beineke. Mechanical resonance damping in an industrial servo drive. In *European Conference on Power Electronics and Applications*, pages 1 – 10, 2007.
- [2] E. Batzies, T. Schöllner, V. Welker, and O. Zirn. Optimal control of direct driven feed axes with flexible structural components. In *Power Electronics and Drive Systems, 2007. PEDS '07*, pages 1127 – 1131, 2007.
- [3] H.P. Beck and D. Turschner. Commissioning of a state-controlled high-powered electrical drive using evolutionary algorithms. *IEEE/ASME Transactions on Mechatronics*, 6:149–154, 2001.
- [4] D.A. Cox, J.B. Little, and D. O’Shea. *Ideals, varieties, and algorithms: an introduction to computational algebraic geometry and commutative algebra*. Undergrad. Texts in Math. Springer, 2007.
- [5] M. Goslar. *Ein Beitrag zur anwendungsorientierten Zustandsregelung elektrischer Hochleistungsantriebe*. PhD thesis, Technische Universität Clausthal, 1998.
- [6] H. Groß, J. Hamann, and G. Wiegärtner. *Electrical feed drives in automation: basics, computation, dimensioning*. Publicis MCD Corporate Pub., 2001. Siemens AG.
- [7] A. Higginson and S. Handley. The self commissioning of high performance servo drives for precision mechanical systems. In *Proceedings. IECON '91., 1991 International Conference on Industrial Electronics, Control and Instrumentation*, volume 1, pages 274 – 279, 1991.
- [8] Zirn. O. and A. Fink. Master-slave state space control for large milling rotary tables. In *8th International Symposium on Advanced Electromechanical Motion Systems & Electric Drives Joint Symposium, 2009. ELECTROMOTION 2009*, pages 1–6, 2009.
- [9] D. Schröder. *Elektrische Antriebe*, volume 2. Springer, 1995.
- [10] B. Sturmfels. *Solving systems of polynomial equations*, volume 97 of *CBMS Reg. Conf. Ser.* Amer. Math. Soc., 2002.
- [11] H. Wertz and F. Schutte. Self-tuning speed control for servo drives with imperfect mechanical load. In *Conference Record of the 2000 IEEE Industry Applications Conference*, volume 3, pages 1497 – 1504. IEEE, 2000.
- [12] O. Zirn. *Machine Tool Analysis: Modelling, Simulation and Control of Machine Tool Manipulators*. ETH Zürich, Department of Mechanical & Process Engineering, 2008. Habilitation Thesis.
- [13] O. Zirn, E. Batzies, S. Weikert, and T. Schöllner. State control of servo drives with flexible structural components. In *Industry Applications Conference, 2006. 41st IAS Annual Meeting. Conference Record of the 2006 IEEE*, volume 4, pages 1760–1766. IEEE, 2006.

- [14] O. Zirn, A. Fink, and V. Welker. Robuste und schwingungsarme Drehzahlregelung für elastische Servoantriebsketten. In *6. VDI-Fachtagung "Schwingungen in Antrieben 2009"*, Leonberg, Germany, 21.-22.10.2009, 2009.
- [15] O. Zirn, A. Monat, and T. Schöller. Control of direct driven feed axes with flexible structural components. In *Conference record IEEE Industrial Applications Society Annual Meeting, Hong Kong*. IEEE, 2005.

HOCHSCHULE FURTWANGEN, FAKULTÄT FÜR COMPUTER & ELECTRICAL ENGINEERING, ROBERT-GERWIG-PLATZ 1, 78120 FURTWANGEN, GERMANY
E-mail address: batzies@hs-furtwangen.de

FACHBEREICH MATHEMATIK UND INFORMATIK, PHILIPPS-UNIVERSITÄT MARBURG, 35032 MARBURG, GERMANY
E-mail address: katthaen@mathematik.uni-marburg.de

FACHBEREICH MATHEMATIK UND INFORMATIK, PHILIPPS-UNIVERSITÄT MARBURG, 35032 MARBURG, GERMANY
E-mail address: welker@mathematik.uni-marburg.de

INSTITUT FÜR PROZESS- UND PRODUKTIONSLEITTECHNIK, TU-CLAUSTHAL, ARNOLD-SOMMERFELD-STR. 1 38678 CLAUSTHAL-ZELLERFELD, GERMANY
E-mail address: oliver.zirn@tu-clausthal.de